NANO LETTERS

2003
Vol. 3, No. 9
1183−1186

Predictions of New Crystalline States for Assemblies of Nanoparticles: Perovskite Analogues and 3-D Arrays of Self-Assembled Nanowires

David P. Stucke and Vincent H. Crespi*

Department of Physics and Materials Research Institute, The Pennsylvania State University, 104 Davey Lab, University Park, Pennsylvania 16802-6300

Received April 15, 2003; Revised Manuscript Received July 14, 2003

ABSTRACT

A genetic search algorithm for optimizing the packing density of self-assembled multicomponent crystals of nanoparticles predicts several new structures with stoichiometries of *AB* (fused spheres), ABC_2, ABC_3, ABC_4 and AB_2C_2. These new structures have hierarchical layered or linear arrangements that could be useful for functional self-assembled systems. For example, the fused-sphere binary crystal assembles with zigzag rows of parallel nanowires. The genetic search suceeds while a comparable stochastic algorithm fails to find any structures better than the well-known unary or binary phase-separated systems.

As increasing attention focuses on structuring materials on the nanometer scale, self-assembly techniques become more prominent. Whereas extended assemblies of monodisperse hard-core spheres form only close-packed lattices, more complex systems containing mixed or fused spheres, layered materials, ellipsoids, rods, or other structures promise a richer panoply of structural types, particularly when building blocks of different sizes are combined.[1] An efficient search algorithm for more complex periodic structures could therefore provide an important tool in the design of complex self-assembled materials. Theoretical guidance toward self-assembly requires a means to efficiently search the very large configuration spaces of extended systems for thermodynamically preferred structures. Here we describe such an algorithm and the results it produces: several new classes of binary and ternary crystals of spherical nanoparticles, including a family of layered perovskite-like systems and an unusual three-dimensional array of parallel zigzag nanowires.

Genetic searches are so-called because they borrow from biology the idea of creating new "child" structures by combining characteristics (i.e., genes) from "parent" structures. In our case, the structures are parameterized by various displacement vectors (defined below), and vectors from each parent are combined to construct a child. A genetic search takes long strides in configuration space. Therefore, the algorithm will work best if the surface defined by the figure of merit (such as a binding energy or packing density) has long valleys oriented along coordinate directions. Geometrically, the merging of structural information from two parent structures into a child, (within an M dimensional configuration space), corresponds to finding the single point of intersection between one m and one $M - m$ dimensional hyperplane, each passing through one parent. If coordinate directions define valleys, then the child has a better probability of sitting near the intersection of two valleys; a subsequent local optimization can then fine-tune the structure before the next generation. Genetic algorithms have already been applied to finite systems such as clusters (C_{60} and Si_n) and point charges on shells.[2] These bounded structures were parameterized with simple lists of atomic coordinates and then bisected in real space and merged to form progeny. This real-space bisection works well for clusters, because the importance of short-range interactions implies that contiguous subsets of atoms (or point charges) from each parent will tend to define valleys. These subsets can be merged sensibly to make progeny, with the new interactions occurring mainly at the surface of fusion.

An extended system such as a crystal cannot be effectively bisected in this way, because the lattice vectors do not define local bond angle or bond length information. Instead, we must find an alternative parameterization of the lattice periodicity, one which propagates local structural information to the next generation. To this end, we represent the crystal as a multi-headed "hydra" H of displacement vectors: $H \equiv (\vec{B}_1, \vec{D}_1, \vec{B}_2, \vec{D}_2, \vec{B}_3, \vec{D}_3, \vec{B}_4, \vec{B}_5, \ldots \vec{B}_N)$. The vectors $\{B\}$ interconnect nearby particles within a single unit cell, and the vectors $\{D\}$ connect particles in adjacent unit cells and

(1) * Corresponding author. http://www.phys.psu.edu/people/crespi.html.

10.1021/nl034230y CCC: $25.00
Published on Web 08/20/2003

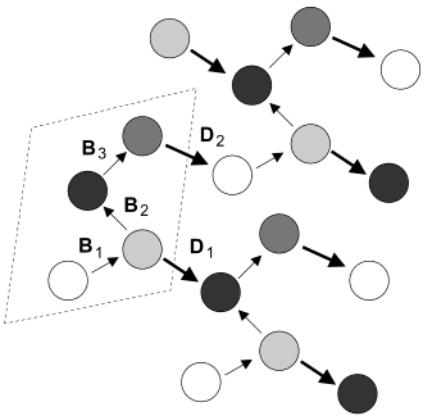

Figure 1. The "hydra" representation of a crystal uses a chain of linked displacement vectors within and between unit cells to enable an efficient exploration of the energy surface. Only two dimensions are shown for clarity. The term "hydra" refers to a body B with D heads extending outward. The gene sequence is, for example, ($\vec{B}_1$, $\vec{D}_1$, $\vec{B}_2$, $\vec{D}_2$, $\vec{B}_3$).

thereby define the periodicity. N is the number of particles in the unit cell. In d dimensional space, the hydra has a total of $Nd + d^2$ elements; (we take $d = 3$). The projections to neighboring unit cells are spread throughout the hydra and always interconnect distinct particles; this allows maximum flexibility in representation while maintaining predominately nearest-neighbor displacements. Since the projections $\{D\}$ to neighboring cells can represent nearest-neighbor interactions (unlike standard lattice vectors), bisecting the hydra and recombining disparate halves tends to preserve the local motifs of proximal interparticle separations and angles; these motifs are the primary determinants of valleys in the fitness surface.[3]

We create a random initial population of structures by concatenating a set of interparticle displacements with random directions and an average length centered about a typical nearest-neighbor separation. This includes the projections $\{D\}$ to adjacent unit cells, so that they also define nearest-neighbor bonds. During this concatenation, any highly unfavorable structures are immediately rejected, provided they do not fall within a predefined minimum fitness threshold.[4] Two parents are chosen at random from this population and mated into a child structure by selecting the first p vectors from hydra H^i and the remaining vectors from H^j and varying the crossover point p randomly from one mating to another. For example: $H^{\text{child}} = H^i \bigstar H^j = (\vec{B}_1^{\,i}, \vec{D}_1^{\,i}, \vec{B}_2^{\,i}, \vec{D}_2^{\,j}, \vec{B}_3^{\,j}, \vec{D}_3^{\,j}, \vec{B}_4^{\,j})$, with a crossover after the third vector. Structural diversity must be maintained from generation to generation to prevent the population from self-trapping as a set of clones within single local minima. We evaluate $\hat{H}^i \cdot \hat{H}^j$, a dot product between two structures (where $\hat{H} = \vec{H}/|\vec{H}|$ is a hydra normalized to an overall length of one) and accept a child into the population only if (i) its maximum normalized dot product against the existing population does not exceed a fixed amount (~ 0.8) and (ii) its absolute fitness difference from all extant structures exceeds a fixed amount ($\sim 0.5\%$ of the typical energy scale for relaxed structures). To broaden the search space, 10 to 20% of bonds suffer a small random fluctuation (mutation) of 5 to 10% (Gaussian standard deviation) in the interparticle separation before the complimentary halves are recombined. Since the joint between the pieces from each parent is arbitrary, we first optimize just the angular orientation of this joint (using the potential function defined below), moving the two respective halves as rigid units. Each child is then fully relaxed to the local energy minimum. Children are generated in batches of 10 to 20 and are inserted into the breeding population if their figures of merit are within those of the top 20 current active structures. The generations proceed, retaining the top 20 structures at each iteration, until a preset number of satisfactory progeny has been generated (typically 100−200 generations).

We apply this algorithm first to crystals formed from hard spherical nanoparticles, because they provide an easily evaluated approximate fitness function. Rather than directly modeling the entropic contributions from interacting hard-core particles, we instead target the packing density as the ultimate figure of merit and use the binding energy from a fictitious two-body hard-core potential (with a long-range attraction) as a surrogate fitness function to generate densely packed structures. The potential $V = \epsilon[(\sigma/r)^m - (\sigma/r)^n]$ with $m = 48$ and $n = 24$ ensures a well-defined sphere radius. The particular m and n chosen have little effect on the final results, so long as the potential has a generic weak longer-ranged attraction and a core hard enough to allow a precise definition of the packing fraction. Although we select on this fictitious binding energy, the final optimized solutions are evaluated based on their packing fraction; we find good agreement with prior results for known crystalline packings. As demonstrated in the seminal early work of Hachisu and Yoshimura,[5] the packing fraction of hard-sphere colloids is a good first approximation for the relative stability of competing colloidal phases, particularly if surface charging effects are relatively weak or highly screened.[6] This figure of merit is also highly computationally efficient, so it is very useful for an initial application of the method.

Calculation of the crystal energy is done through the summing pair interactions between particles. The energy calculation is done over all particle pairs within a finite block of unit cells to encourage formation of compact sets of basis/lattice vectors.[7] As a test, we first search for the known densely packed unary and binary structures A, AB, and AB_2 formed from spherical constituents.[8] In all cases, including artificial supercells up to 10 formula units, the genetic search finds the correct solution. (For all of our calculations, including the binary and ternary calculations to be described below, a similar potential was used, with a constant well depth and an equilibrium pair separation equal to the sum of the radii of the two relevant spheres.) A competing random search, which uses the same initial structure generation and local optimization as the genetic search, ranges from 3 to 100 times slower, with the slowest performance in the larger cells. For supercell binary systems the random search failed in all runs. The genetic algorithm is superior, particularly for the more richly structured systems, because it can retain and exploit preferred structural motifs. We next search in previously unexplored systems such as ternary sphere

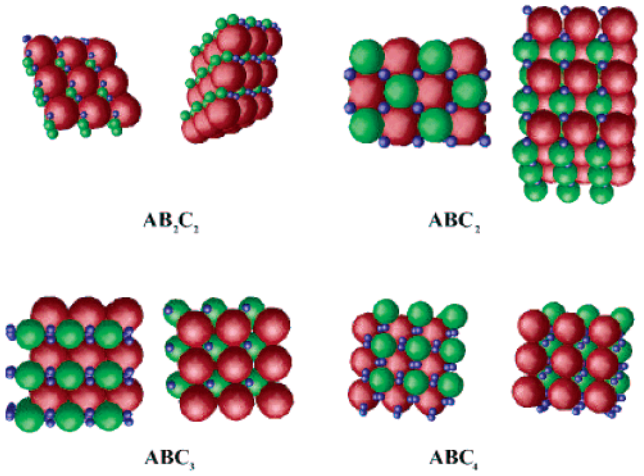

Figure 2. Preferred self-assembled ternary structures (two views of each).

compounds and fused sphere pairs; fusion of sphere pairs frustrates phase separation and could force the formation of novel structures. Specifically, we study *ABC*, ABC_2, AB_2C_2, ABC_3, ABC_4, and fused *AB* systems, covering the range of relative R_B/R_A and R_C/R_A size ratios from 0.2 to 0.9. Following, for example, Hachisu and Yoshimura,[5] the candidate structures' packing fractions were compared to the maximal packing fraction possible among the appropriate ratios of known unary and binary sphere crystals (e.g., FCC ≈ 0.74, NaCl (AB) ≈ 0.793, CsCl (AB) ≈ 0.73, AlB_2 (AB_2) ≈ 0.78) in the applicable size regimes for each structure.

In all cases except *ABC* we find new structures that are higher in packing density than the competing phase-separated systems. Due to computational constraints, for the ternary systems we study a single formula unit per unit cell; for the fused dimer case we study both one- and two-formula units. Because structures of higher packing efficiency could exist with more formula units per cell, the results here provide a lower bound on the range of (R_B/R_A, R_C/R_A) phase space in which novel crystals could be found.

The $ABC_{2/3/4}$ stoichiometries form a closely related family of layered tetragonal or orthorhombic structures. In the archetypal ABC_2, the largest (*A*) spheres contact each other in a two-dimensional square lattice; the medium (*B*) spheres then fill the depressions within this layer, while the smallest (*C*) spheres fill the gaps between the *B* spheres; (see Figure 2). For ABC_2 the *B*-*C* layers have the structure of a Cu−O perovskite plane and attain a highest packing fraction of 0.78 when $R_a = 1.0$, $R_b = 0.72$, and $R_b = 0.28$. For comparison, the close-packed packing fraction is 0.74. These optimal sizes yield a simple commensurability: $R_a = R_b + R_c$ and the *A*-sublattice body diagonal of $\sqrt{3}$ leaves holes of $\sqrt{3} - 1 \approx 0.73$ to be filled by *B* spheres. ABC_3 and ABC_4 differ from ABC_2 in having different arrangements of the *C* spheres (see Figure 3). The familial similarities suggest that the overall *A*−*B* framework is rather robust and that a real system may contain a multiphase mixture of *C* placements.[9] Similar to the known binary colloidal structures, these ternary systems tend to build around certain special commensurations between the constituents.

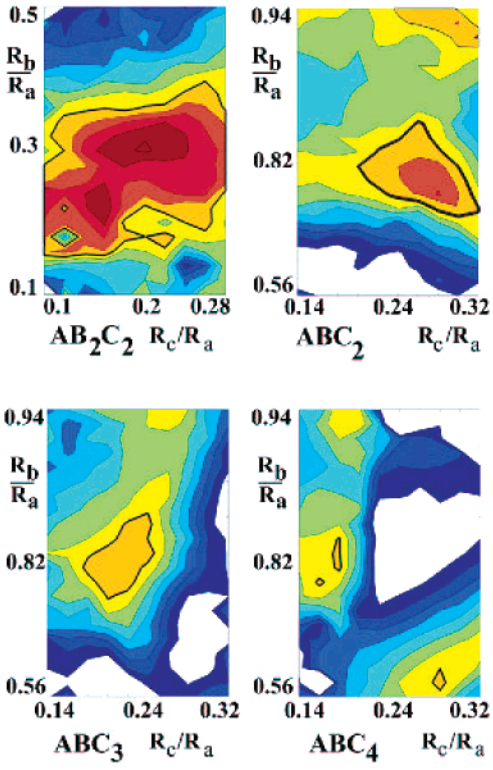

Figure 3. Packing densities of ternary crystals of spherical nanoparticles. The region within the thick lines has higher packing efficiency than phase separated competitors.

In contrast, AB_2C_2 forms distorted triangular-packed layers of large spheres with the medium and small spheres filling in the gaps. This structure attains an optimal packing fraction of 0.77 at $R_b/R_a = 0.24$ and $R_c/R_a = 0.16$. The proximity of the *A* sublattice to close packing explains the wide range over which this structure has a high packing efficiency (see Figure 3). Both families of ternary structures exhibit layering, which may facilitate applications that require the isolation of distinct subunits, such as self-assembled circuits or waveguides.[10] The contour plots are very smooth. Although each point on this surface results from an independent genetic search, the packing densities of the resulting optimal structures form a smooth manifold. Since it is unlikely that the search would always find the same smooth continuous family of (nonglobal) local minima, the smoothness of the contours provides strong heuristic evidence that the algorithm is finding the global optimum.

The fusion of spheres into nanoparticle "molecules" frustrates phase separation and provides an interesting mechanism to induce novel structures. *AB* stoichiometry spheres show several well-known phases: around $R_b/R_a \sim 0.22$, 0.41, and 0.73 the system prefers the ZnS, NaCl/NiAs, and CsCl structures, respectively. The range from 0.5 to 0.65 has poor packing efficiency and therefore holds greatest promise for novel structural accommodations if phase separation is frustrated by fusion. In this range, we find a new self-assembled $(AB)_2$ structure wherein the larger spheres form a staggered but impenetrable layer, with the smaller spheres tilting cross-wise into paired zigzag wires that run in well-separated parallel rows. This interesting structure is

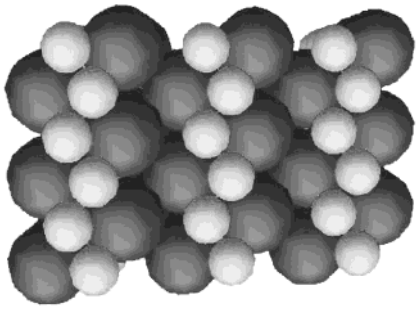

Figure 4. Preferred structure for a fused-sphere system. The smaller spheres align to form self-assembled zigzag nanowires (R_b/R_a = 0.58).

preferred over a wide range of R_b/R_a (0.5−0.65), assuming a unit cell containing two dimer pairs. These self-assembled zigzag rows could either form nanowires themselves (if the small spheres are metallic) or provide a template for the arrangement of additional nanorods onto the crystal's surface. A competing structure (but with a slightly smaller packing fraction) in which the smaller spheres are separated is also observed. The nanowire structure could be further favored by adding a small attractive contact interaction between the smaller spheres.

Once these target dense-packed structures are known, one could further encourage their formation by chemical functionalization of the particle surfaces to produce explicit nearest-neighbor interactions that reinforce the preferred contacts. The algorithm is straightforward to parallelize and therefore could be extended to handle more computationally intensive figures of merit,[11] such as self-consistent density functional total energy calculations for atomic-scale crystals or screened electrostatic effects in colloidal crystals with strong surface charge. The ability to predict promising parameter regimes for the self-assembly of extended periodic systems should aid in the search for new materials with interesting electrical, optical, or chemical properties.

Acknowledgment. We gratefully acknowledge support from the Packard Foundation and the National Science Foundation under the auspices of the Penn State Materials Research Science and Engineering Center and grant DMR-9876232.

References

(1) Yin, Y.; Lu, Y.; Xia, Y. *J. Am. Chem. Soc.* **2001**, *123*, 771−772. Yin, Y.; Lu, Y.; Gates, B.; Xia Y. *J. Am. Chem. Soc.* **2001**, *123*, 8718−8729. Velikov, K. P.; Christova, C. G.; Dullens, R. P. A.; van Blaaderen, A. *Science* **2002**, *296*, 106−109. Jiang, P.; Bertone, J. F.; Colvin, V. L. *Science* **2001**, *291*, 453−457; Johnson, S. A.; Olliver, P. J.; Mallouk, T. E. *Science* **1999**, *283*, 963−965. Wu, H.; Thalladi, V. R.; Whitesides, S.; Whitesides, G. M. *J. Am. Chem. Soc.* **2002**, *124*, 14495−14502. Douglas, T.; Young, M. *Adv. Mater.* **1999**, *11*, 679−685. Yun, C. C.; Major, J. L.; Strouse, G. F.; Leon, R.; Noetzel, R.; Fafared, S.; Huffaker, D. *Mater. Res. Soc. Symp. Proc.* **2001**, *642*, J7.8. Murray, C. B.; Kagan, C. R.; Bawendi, M. G. *Annu. Rev. Mater. Sci.* **2000**, *30*, 545−610.

(2) Deaven, D. M.; Ho, K. M. *Phys. Rev. Lett.* **1995**, *75*, 288−291. Ho, K. M.; Shvartsburg, A. A.; Pan, B.; Lu, Z.; Wang, C.; Wacker, J.; Fye, J. L.; Jarrold, M. *Nature* **1998**, *392*, 582−585. Morris, J. R.; Deaven, D. M.; Ho K. M. *Phys. Rev. B* **1996**, *53*, R1740−R1743.

(3) Whitley, D.; Rana, S.; Heckendorn, R. B. *J. Comput. Inf. Technol.* **1999**, *85*(1−2), 245−276.

(4) Generally, the threshold was set so that structures with a positive binding energy were rejected before local relaxation. This criterion is fairly restrictive. However, since structure generation is very fast, the overall algorithm is most efficient when the input structures to the local relaxation are sufficiently stable that structural motifs are reasonably well preserved during the local relaxation.

(5) Hachisu, S. and Yoshimura, S. *Physics of Complex and Supermolecular Fluids*; Wiley: New York, 1987; p 221. Hachisu, S.; Yoshimura, S. *Nature* **1980**, *283*, 188−189.

(6) Of course, packing fraction as a figure of merit does not contain the more subtle higher-order entropic effects that can distinguish structures of identical packing fraction, such as fcc and hcp. Cottin, X.; Monson, P. A. *J. Chem. Phys.* **1995**, *102*, 3354−3360.

(7) The most efficient way to evaluate the potential would seem to be as a sum of pair contributions outward from a single central unit cell to a cutoff distance (rather than to evaluate all pairwise interactions in a finite block of unit cells, as we did). The set of all particles that lie within this cutoff could apparently be constructed by finding the particles associated with every unit cell in some large $M \times M \times M$ box of unit cells surrounding the central cell, and then retaining all such particles that fall within the cutoff distance. However, one's intuition fails here: the genetic algorithm can produce structures with very long basis vectors, so that the $M \times M \times M$ box does *not* generate all particles in the neighborhood of the central cell. In particular, the algorithm can generate pathological structures with very long basis vectors that are comparable in length to M times a lattice vector. In such a case, the $M \times M \times M$ construction misses some particles so that the unit cells near the center of the box are not identically populated. Specifically, the central cell is "missing" one particle, and that particle, which is present in one or more neighboring cells, yields spurious coordination numbers. This pathology, which is avoided by summing interactions over all pairs within an entire block of unit cells, is actually a testament to the thoroughness of the genetic search.

(8) Sanders, J. V. *Philos. Mag. A* **1980**, *42*, 705−720. Murray, M. J.; Sanders, J. V. *Philos. Mag. A* **1980**, *42*, 721−740. Pusey, P. N.; van Megen, W. *Nature* **1986**, *320*, 340−342. Bartlett, P.; Ottewill, R. H.; Pusey, P. N. *Phys. Rev. Lett.* **1992**, *68*, 3801−3804. Hunt, N.; Jardine, R.; Bartlett, P. *Phys Rev. E* **2000**, *62*, 900−913.

(9) Alternatively, the C particles may occupy the location of the perovskite apical oxygens in the ABC_3 or ABC_4 structures, in which case size ratios close to the optimal ABC_2 values, (R_A, R_B, R_C) = (1.0, 0.72, 0.28), may be preferred.

(10) Rengarajan, R.; Jiang, P.; Larrabee, D. C.; Colvin, V. L.; Mittlemen M. *Phys. Rev. B* **2001**, *64*, 205103-1−205103-4. Vlasov, Y. A.; Astratov V. N.; Baryshev A. V. *Phys. Rev. E* **2000**, *61*, 5784−5793.

(11) Bazterra, V. E.; Ferraro, M. B.; Facelli J. C. *J. Chem. Phys.* **2002**, *116*, 5984−5991. Bazterra, V. E.; Ferraro, M. B.; Facelli J. C. *J. Chem. Phys.* **2002**, *116*, 5992−5995.

NL034230Y